Fast 3D Isotropic Proton Density-Weighted Fat-Saturated MRI of the Knee at 1.5 T with Compressed Sensing: Comparison with Conventional Multiplanar 2D Sequences

Schnelle 3D-isotrope protonengewichtete fettunterdrückte MRT des Kniegelenks bei 1,5 Tesla mit Compressed Sensing: Vergleich mit konventionellen multiplanaren 2D-Sequenzen

Authors

Christoph H.-J. Endler[1, 2], Anton Faron[1, 2], Alexander Isaak[1, 2], Christoph Katemann[3], Narine Mesropyan[1, 2], Patrick A. Kupczyk[1, 2], Claus C. Pieper[1], Daniel Kuetting[1, 2], Dariusch R. Hadizadeh[1], Ulrike I. Attenberger[1], Julian A. Luetkens[1, 2]

Affiliations

1 Department of Diagnostic and Interventional Radiology, University Hospital Bonn, Germany
2 Quantitative Imaging Lab Bonn (QILaB), University Hospital Bonn, Germany
3 Philips Healthcare, Hamburg, Germany

Key words

3D sequence, knee imaging, MRI, meniscal tear, compressed sensing

received 15.10.2020
accepted 09.12.2020
published online 03.02.2021

Bibliography

Fortschr Röntgenstr 2021; 193: 813–821
DOI 10.1055/a-1337-3351
ISSN 1438-9029

Georg Thieme Verlag KG, Rüdigerstraße 14, 70469 Stuttgart, Germany

Correspondence

PD Dr. med. Julian Luetkens
Department of Diagnostic and Interventional Radiology, University Hospital Bonn, Venusberg-Campus 1, 53127 Bonn, Germany
julian.luetkens@ukbonn.de

ZUSAMMENFASSUNG

Ziel Compressed Sensing (CS) ist eine Signalverarbeitungstechnik, mithilfe derer man durch Unterabtasten des k-Raums weniger Daten akquirieren und so MRT-Aufnahmen beschleunigen kann. Ziel dieser prospektiven Studie war die Klärung der Frage, ob eine 3-dimensionale (3D) isotrope protonengewichtete fettgesättigte Sequenz (PDwFS) mit CS konventionelle multidirektionale 2-dimensionale (2D) Sequenzen bei 1,5 T ersetzen kann.

Material und Methoden 20 Patienten (45,2 ± 20,2 Jahre; 10 Frauen) mit Verdacht auf Kniebinnenschaden erhielten am 1,5T-MRT zusätzlich zu den konventionellen, in 3 Ebenen angefertigten 2D-PDwFS (Akquisitionszeit: 4:05min + 3:03min + 4:46min = 11:54 min) eine 3D-PDwFS mit CS-Beschleunigungsfaktor 8 (Akquisitionszeit: 4:11 min). Die Homogenität der Fettunterdrückung, die Bildschärfe und Artefakte wurden anhand von 5-Punkt-Likert-Skalen durch 2 erfahrene Radiologen beurteilt. Anhand der so vergebenen Punkte wurde die Gesamtbildqualität ermittelt. Zusätzlich wurden quantitative Kontrastverhältnisse für die Menisken (MEN), das vordere (ACL) und das hintere Kreuzband (PCL) im Vergleich zum Musculus popliteus errechnet.

Ergebnisse Die Gesamtbildqualität wurde in der 3D-PDwFS höher als in den 2D-PDwFS-Sequenzen bewertet (14,45 ± 0,83 vs. 12,85 ± 0,99; $p < 0,01$), insbesondere aufgrund weniger Artefakte (4,65 ± 0,67 vs. 3,65 ± 0,49; $p < 0,01$) und einer homogeneren Fettunterdrückung (4,95 ± 0,22 vs. 4,55 ± 0,51; $p < 0,01$). Die Bildschärfe ergab keinen signifikanten Unterschied (4,80 ± 0,41 vs. 4,65 ± 0,49; $p = 0,30$). Die quantitativen Kontrastverhältnisse waren in den 3D-PDwFS für alle gemessenen Strukturen höher als in den 2D-PDwFS (MEN: $p < 0,05$; ACL: $p = 0,06$; PCL: $p = 0,33$). In einem Fall konnte ein Meniskusriss lediglich mithilfe einer multiplanaren Reformatierung der 3D-PDwFS diagnostiziert werden und wäre auf den konventionellen multiplanaren 2D-Sequenzen übersehen worden.

Schlussfolgerung Eine isotrope fettgesättigte 3D-PD-Sequenz mit CS ermöglicht eine schnelle und qualitativ hochwertige 3D-Bildgebung des Kniegelenks bei 1,5 T und könnte konventionelle multiplanare 2D-Sequenzen ersetzen. Neben einer schnelleren Bildakquise bietet die 3D-Sequenz Vorteile in der Bildgebung kleiner Strukturen.

Kernaussagen:

- 3D-PDwFS mit Compressed Sensing ermöglicht eine 3-fach schnellere Knie-Bildgebung verglichen mit multiplanaren 2D-Sequenzen.

- 3D-PDwFS mit Compressed Sensing ermöglicht eine qualitativ hochwertige Knie-Bildgebung bei 1,5 T.
- Isotrope 3D-Sequenzen bieten Vorteile in der Darstellung kleiner Strukturen durch die Möglichkeit der multiplanaren Reformation.

ABSTRACT

Purpose Compressed sensing (CS) is a method to accelerate MRI acquisition by acquiring less data through undersampling of k-space. In this prospective study we aimed to evaluate whether a three-dimensional (3D) isotropic proton density-weighted fat saturated sequence (PDwFS) with CS can replace conventional multidirectional two-dimensional (2D) sequences at 1.5 Tesla.

Materials and Methods 20 patients (45.2 ± 20.2 years; 10 women) with suspected internal knee damage received a 3D PDwFS with CS acceleration factor 8 (acquisition time: 4:11 min) in addition to standard three-plane 2D PDwFS sequences (acquisition time: 4:05 min + 3:03 min + 4:46 min = 11:54 min) at 1.5 Tesla. Scores for homogeneity of fat saturation, image sharpness, and artifacts were rated by two board-certified radiologists on the basis of 5-point Likert scales. Based on these ratings, an overall image quality score was generated. Additionally, quantitative contrast ratios for the menisci (MEN), the anterior (ACL) and the posterior cruciate ligament (PCL) in comparison with the popliteus muscle were calculated.

Results The overall image quality was rated superior in 3D PDwFS compared to 2D PDwFS sequences (14.45 ± 0.83 vs. 12.85 ± 0.99; $p < 0.01$), particularly due to fewer artifacts (4.65 ± 0.67 vs. 3.65 ± 0.49; $p < 0.01$) and a more homogeneous fat saturation (4.95 ± 0.22 vs. 4.55 ± 0.51; $p < 0.01$). Scores for image sharpness were comparable (4.80 ± 0.41 vs. 4.65 ± 0.49; $p = 0.30$). Quantitative contrast ratios for all measured structures were superior in 3D PDwFS (MEN: $p < 0.05$; ACL: $p = 0.06$; PCL: $p = 0.33$). In one case a meniscal tear was only diagnosed using multiplanar reformation of 3D PDwFS, but it would have been missed on standard multiplanar 2D sequences.

Conclusion An isotropic fat-saturated 3D PD sequence with CS enables fast and high-quality 3D imaging of the knee joint at 1.5 T and may replace conventional multiplanar 2D sequences. Besides faster image acquisition, the 3D sequence provides advantages in small structure imaging by multiplanar reformation.

Key Points:

- 3D PDwFS with compressed sensing enables knee imaging that is three times faster compared to multiplanar 2D sequences
- 3D PDwFS with compressed sensing provides high-quality knee imaging at 1.5 T
- Isotropic 3D sequences provide advantages in small structure imaging by using multiplanar reformations

Citation Format

- Endler CH, Faron A, Isaak A et al. Fast 3D Isotropic Proton Density-Weighted Fat-Saturated MRI of the Knee at 1.5 T with Compressed Sensing: Comparison with Conventional Multiplanar 2D Sequences. Fortschr Röntgenstr 2021; 193: 813–821

Introduction

Magnetic resonance imaging (MRI) of the knee is one of the most frequently performed MRI examinations in musculoskeletal imaging. It is the most accurate imaging method for the detection of intra-articular pathologies due to its excellent soft-tissue contrast and also enables a comprehensive evaluation of osseous structures, making it indispensable in the orthopedic evaluation.

Due to the acquisition of thin continuous sections and the lack of interslice gaps, three-dimensional (3D) sequences offer many advantages in joint imaging compared to multidirectional two-dimensional (2D) sequences. These include decreased partial volume averaging, a reduction of pulsation artifacts, accurate volumetric quantification, and a greater signal compared to conventional 2D sequences. Several studies were already able to prove a comparability or even superiority of 3D sequences over conventional standard multiplanar 2D sequences [1–4]. One of the main advantages of isotropic 3D sequences is the possibility of thin multiplanar reformations (MPRs) in arbitrary orientations. It is possible to accurately visualize small structures that otherwise would require additional, specifically angulated orientations in conventional multiplanar sequences. These additional sequences are not only time-consuming, but also require exact adjustments at the scanner. The main limitation of 3D sequences is their long acquisition time which leads to an increased sensitivity for motion artifacts and thereby prevents its wide acceptance in musculoskeletal imaging [5]. There have been different approaches to accelerate image acquisition in 3D data sets, including longer echo train lengths, the use of higher linear parallel imaging (PI) acquisition factors, larger voxel sizes, and decreased flip angles [5]. However, these adjustments can result in a loss of image quality due to increased image noise, loss of uniformity of the image quality using MPR and blurring, which can lead to limited diagnostic accuracy for meniscal tears and cartilage defects [3, 6]. It took until 2007 for a clinically practicable scan time of 7:20 minutes to be achieved with a 3D fast spin echo (FSE) sequence [7]. However, various authors agreed that an acceptable scan time of 5 minutes or less would be required for 3D sequences to be helpful in the clinical routine [3, 4, 8, 9].

The introduction of compressed sensing (CS) may prove helpful to develop reliable robust and especially fast sequences as required [10]. CS acquires less data through sparsity and incoherent undersampling of k-space, followed by a nonlinear iterative reconstruction to correct for sub-sampling artifacts. Since the introduction of CS, it has been implemented into clinical protocols for many different applications and anatomic regions [11–13].

However, only a limited number of studies have used CS in musculoskeletal imaging [11, 12, 14–16], and only a few studies have shown its feasibility in knee imaging, all at 3 Tesla (T) [8, 17–20]. While an acceleration of image acquisition or an improvement of image quality can be achieved at 3 T, the combination of CS and 3D imaging is not limited to a specific magnetic field strength.

The purpose of this study was therefore to evaluate image quality and lesion detectability of an isotropic 3D proton density-weighted fat-saturated (PDwFS) sequence of the knee using CS with an acceleration factor of 8 at 1.5 T in comparison to conventional multiplanar 2D sequences.

Materials and Methods

This prospective single-center study was approved by the institutional ethics commission. Written informed consent for the acquisition of an additional 3D sequence was obtained from all subjects prior to examination. One author is an employee of Philips Healthcare. This author was involved neither in the study design nor in the control of data.

Study population

20 consecutive patients with a clinical indication for MRI based on the suspicion of internal knee damage were included in the study. The mean age was 45.2 ± 20.2 years; range: 18–82 years (10 male patients [36.3 ± 14.4 years, range: 19–59 years]; 10 female patients [54.0 ± 21.9 years, range: 18–82 years]; p = 0.07). Examinations between June and October 2019 were included. Inclusion criteria were: 1) suspicion of internal knee damage, 2) ≥ 18 years of age. Exclusion criteria were: 1) contraindications for MRI like metallic implants, pacemakers or claustrophobia and 2) indications for contrast-enhanced MRI. Patient characteristics were retrieved using the clinical information system. An overview of the patient characteristics, the MRI indications, and the detected injuries are given in ▶ **Table 1**.

Image acquisition

The MRI scans were performed on a 1.5 T whole-body MR system equipped with a 16-channel knee coil to cover the entire knee (Ingenia, Philips Healthcare, Best, The Netherlands). Examinations were performed feet-first in supine position. In addition to standard 2D PDwFS turbo spin echo (TSE) sequences acquired on three planes (acquisition times: 4:03 min + 3:03 min + 4:46 min = 11:52 min), a 3D PDwFS TSE sequence with CS (acceleration factor 8) was performed at the end of the examinations (acquisition time: 4:11 min). The employed CS technique was based on a combination of compressed sensing and parallel imaging using SENSE (Compressed SENSE, Philips Healthcare, Best, The Netherlands). Post-acquisition coronal and axial MPRs were acquired using the scanner software.

The total acquisition time for both 2D and 3D sequences therefore was 16:03 min. 2D and 3D PD sequences were acquired using a spectral selective attenuation recovery fat saturation technique (SPIR in 2D images, SPAIR in 3D images). All examinations were completed in the same session. MRI scan parameters are given in ▶ **Table 2**.

▶ **Table 1** Patient characteristics, MRI indications, and detected knee injuries for the whole study population. Continuous variables are given as mean±standard deviation, and dichotomous variables as absolute frequency with percentages in parentheses.

▶ **Tab. 1** Patientencharakteristiken, MRT-Indikationen und diagnostizierte Knieverletzungen der Studienteilnehmer. Kontinuierliche Variablen werden als Durchschnitt ± Standardabweichung angegeben, dichotome Variablen als absolute Häufigkeit mit Prozentzahlen in Klammern.

variable	study population (n = 20)
demographics	
age (years)	45.2 ± 20.2
female patients	10 (50 %)
main MRI indications	
obscure knee pain	8 (40 %)
suspicion of meniscal tear	6 (30 %)
suspicion of cruciate ligament rupture	2 (10 %)
others	4 (20 %)
detected knee injuries	
meniscal tear	16 (80 %)
cartilage damage	5 (25 %)
occult fractures	5 (25 %)
collateral ligament injury	4 (20 %)
tendon injury	2 (10 %)
cruciate ligament injury	2 (10 %)
cyclops lesions	1 (5 %)
medial patellofemoral ligament injury	1 (5 %)

Image analysis

Image analysis was performed on a dedicated workstation (IMPAX EE, AGFA HealthCare, Mortsel, Belgium).

Qualitative image analysis

Artifacts, image sharpness, and homogeneity of fat saturation were rated by two experienced, blinded board-certified readers (J.L. (rater 1) and P.K. (rater 2) with 8 and 9 years of experience in musculoskeletal MRI, respectively). Analogous to a previously described approach [1], 5-point Likert scales were used to rate artifacts, image sharpness, and homogeneity of fat saturation as follows:

- artifacts (1: non-diagnostic; 2: poor = insufficient diagnostic confidence; 3: moderate = some artifacts, not interfering with diagnosis; 4: good = minimal artifacts; 5: excellent = no artifacts),
- image sharpness (1: non-diagnostic = blurry; 2: poor = knee structures can be identified, insufficient diagnostic confidence; 3: moderate = sufficient for diagnosis, but low diagnostic confidence; 4: good = diagnostic with high diagnostic confidence; 5: excellent = crispy images) and

▶ **Table 2** Scan protocol with sequence parameters of the applied 2D- and 3D-PDwFS at 1.5 Tesla.

▶ **Tab. 2** Scan-Protokoll mit Sequenzparametern der angewandten 2D- und 3D-PDwFS bei 1,5 Tesla.

parameter	2D PDwFS sagittal	2D PDwFS coronal	2D PDwFS transverse	3D PDwFS
TR/TE (ms)	3323/30	4059/30	5021/30	900/86
flip angle (degrees)	90	90	90	90
field of view (mm)	160 × 160	160 × 160	150 × 150	160 × 160
Matrix	212 × 212 × 29	328 × 269 × 30	320 × 250 × 36	212 × 457
Voxel size (mm)				
▪ acquired	0.48 × 0.56 × 3.00	0.49 × 0.60 × 3.00	0.47 × 0.60 × 3.00	0.75 × 0.75 × 0.75
▪ reconstructed	0.31 × 0.31 × 3.00	0.33 × 0.33 × 3.00	0.31 × 0.31 × 3.00	0.36 × 0.36 × 0.38
slices	29	30	36	360
TSE factor	6	10	10	19
acquisition time (min:s)	4:02.6	3:02.7	4:46.2	4:11.1
PI reduction factor (SENSE)	1.3	1.0	1.8	–
CS factor	–	–	–	8
NSA	1	1	2	1
water-fat shift	1.200 pixels (181.0 Hz/pixel)	0.780 pixels (279.2 Hz/pixel)	0.784 pixels (277.0 Hz/pixel)	0.735 pixels (295.5 Hz/pixel)
fat suppression	SPIR	SPIR	SPIR	SPAIR

PDwFS = proton density-weighted fat-suppressed sequence; PI = parallel imaging; CS = compressed sensing; NSA = number of signal averages; SPAIR = spectral attenuated inversion recovery; SPIR = spectral presaturation with inversion recovery; TR = time of repetition; TE = time to echo; TSE = turbo spin echo; min = minutes; s = seconds.

- homogeneity of fat suppression (1 = non-diagnostic; 2: poor = central and peripheral inhomogeneities; 3: moderate = major inhomogeneities (central); 4: good = minor inhomogeneities (peripheral); 5: excellent = no inhomogeneities).

For intra- and inter-rater reproducibility measurements, all ratings of artifacts, image sharpness, and homogeneity of fat saturation were performed by rater 1 and 2 and were repeated by rater 1. For the calculation of the final score, however, a consensus reading was held in cases of discrepancy. Based on the sum of these ratings, overall image quality scores were generated (a + b + c; 13–15 points: excellent; 10–12 points: good; 7–9 points: moderate; 3–6 points = poor).

Furthermore, all detected internal knee injuries were evaluated in both sequences in consensus by the same two board-certified readers.

Quantitative image analysis

For quantitative analysis, contrast ratios (CR) were measured for the anterior cruciate ligament (ACL), the posterior cruciate ligament (PCL), and the meniscus (MEN) and compared to the signal of the popliteal muscle (CR = (A-B)/A). Preferably large regions of interest (ROI) were placed into the respective structures and signal intensities were measured in the medial portion of the ACL and PCL as well as in the inner meniscus. Signal intensities were also measured in the proximal popliteal muscle next to the inner meniscus. ROIs were placed by the same reader (C.E.) to warrant consistency.

Statistical analysis

SPSS Statistics (version 26; IBM, Armonk, NY) was used for statistical analysis. Participant characteristics and image quality scores are presented as means ± standard deviation (SD) or as percent to absolute frequency. Continuous variables between two groups were compared by using the Mann-Whitney U test. Dichotomous variables were compared by using the Chi-squared test (with a cell count greater than five) or Fisher exact test (with a cell count less than or equal to five). Intra- and inter-rater reproducibility of ratings of artifacts, image sharpness, and homogeneity of fat saturation was assessed using intraclass correlation coefficient (ICC) estimates. ICC estimates and their 95 % confident intervals (CI) were based on a single measurement, absolute agreement, 2-way mixed-effects model. Single measure coefficients are reported. A p-value lower than 0.05 was considered statistically significant.

Results

All examinations were successfully completed by the participants of the study.

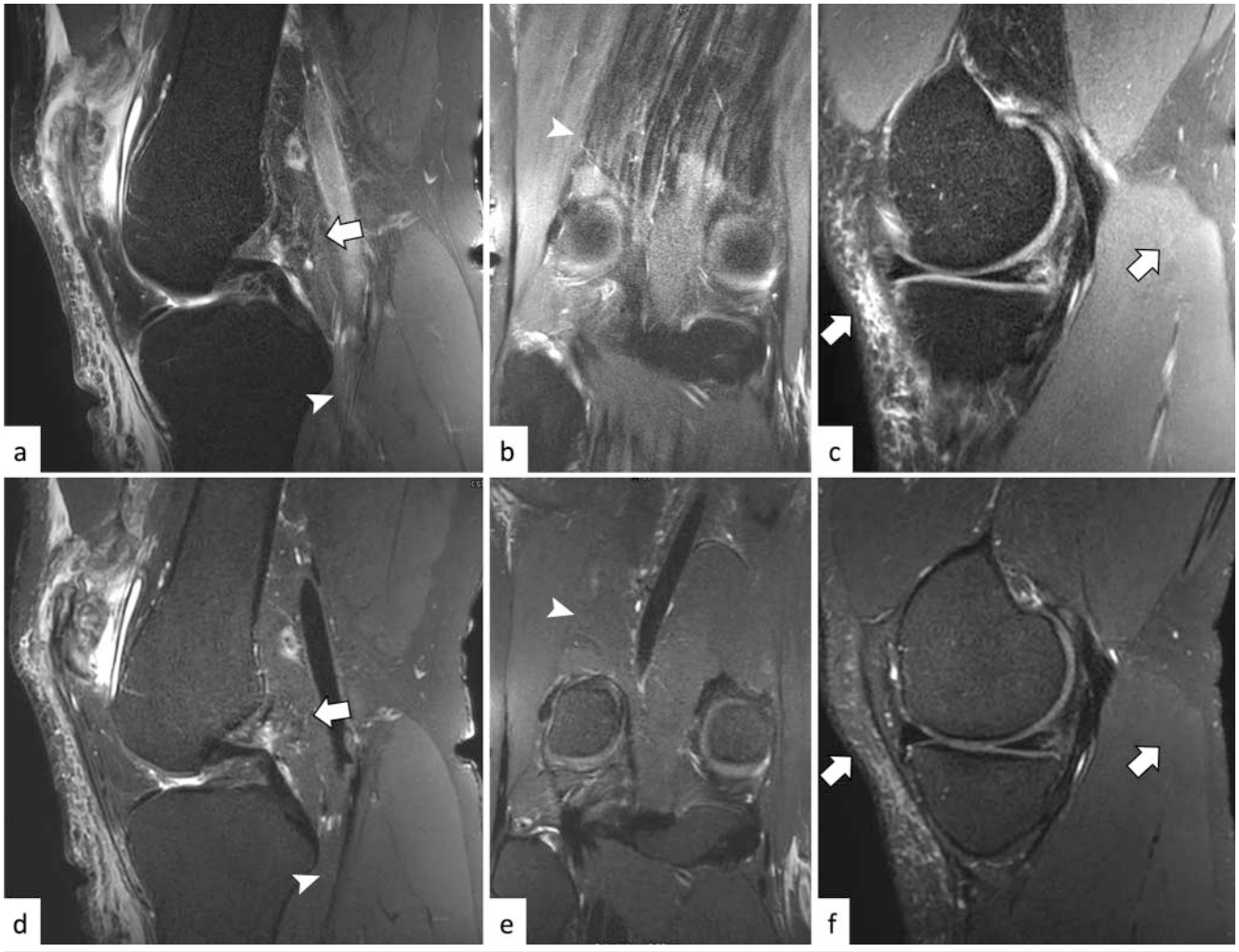

▶ **Fig. 1** Comparison of three-dimensional (3D) isotropic proton density-weighted fat-saturated sequence (PDwFS) with two-dimensional (2D) PDwFS. Note that there are fewer artifacts (arrowheads) and more homogeneous fat saturation (arrows) in the 3D PDwFS (**d–f**; **d** and **f**: sagittal, **e**: coronal) compared to the 2D PDwFS (**a–c**; **a** and **c**: sagittal; **b**: coronal).

▶ **Abb. 1** Vergleich der 3-dimensionalen (3D) isotropen protonengewichteten fettgesättigten Sequenz (PDwFS) mit den 2-dimensionalen (2D) PDwFS. In der 3D-PDwFS sind weniger Artefakte (Pfeilspitzen) und eine homogenere Fettunterdrückung (Pfeile) (**d–f**; **d** und **f**: sagittal, **e**: koronal) im Vergleich zu den 2D-PDwFS (**a–c**; **a** und **c**: sagittal; **b**: koronal) zu beobachten.

Image quality scores for artifacts (4.65 ± 0.67 vs. 3.65 ± 0.49; $p < 0.01$) and homogeneity of fat saturation (4.95 ± 0.22 vs. 4.55 ± 0.51; $p < 0.01$) were superior in the 3D PDwFS MPRs compared to the 2D PDwFS sequences, indicating fewer artifacts and more homogeneous fat suppression in 3D MPRs (▶ **Fig. 1**). There was no significant difference regarding image sharpness (4.80 ± 0.41 vs. 4.65 ± 0.49; $p = 0.30$). Hence, the overall image quality was superior in 3D PDwFS compared to 2D PDwFS imaging (14.40 ± 0.99 vs. 12.85 ± 0.99; $p < 0.01$) (▶ **Table 3**). Analysis of intra- and inter-rater reproducibility (ICC, single measures) of ratings of artifacts, image sharpness, and homogeneity of fat saturation revealed good or excellent results (inter: artifacts: 0.901, 95 % CI: 0.814–0.948, image sharpness: 0.835, 95 % CI: 0.689–0.912, homogeneity of fat saturation: 0.774, 95 % CI: 0.573–0.880; intra: 0.904, 95 % CI: 0.862–0.933).

Quantitative contrast ratios for the menisci and the anterior cruciate ligament were significantly superior in the 3D PDwFS MPRs compared to the 2D PDwFS sequences (MEN: 0.71 ± 0.11 vs. 0.60 ± 0.21; $p < 0.05$ and ACL: 0.43 ± 0.36 vs. 0.19 ± 0.43; $p = 0.06$). The contrast ratios for the posterior cruciate ligament were comparable (0.67 ± 0.13 vs. 0.61 ± 0.24, $p = 0.33$) (▶ **Table 4**).

In total 36 knee injuries were diagnosed; a more detailed overview is given in ▶ **Table 1**. Only two patients underwent arthroscopy, during which the diagnosed internal knee injuries (a loose intraarticular body, synovitis, a rupture of the medial patellar retinaculum, and a retropatellar cartilage defect) could be verified. One oblique meniscal tear (parrot-beak tear) of the lateral meniscus adjacent to the meniscal root could only be identified clearly on 3D PDwFS MPRs (▶ **Fig. 2**) and would have been missed on the standard multiplanar 2D sequences. Except for that meniscal tear,

▶ **Table 3** Parameters of image quality of 2D- and 3D-PDwFS. Overall image quality was higher in 3D-PDwFS sequences with significantly fewer artifacts and more homogeneous fat suppression. Scores for image sharpness were higher in 3D-PDwFS, although not significantly. Continuous variables are given as mean ± standard deviation (top line) and as median with range in parentheses (lower line).

▶ **Tab. 3** Parameter der Bildqualität der 2D- und 3D-PDwFS. Die Gesamtbildqualität war in der 3D-PDwFS höher mit signifikant weniger Artefakten und einer homogeneren Fettunterdrückung. Die Bildschärfe wurde in der 3D-PDwFS nicht signifikant höher bewertet. Kontinuierliche Variablen werden als Durchschnitt ± Standardabweichung (jeweils obere Zeile) und als Median mit Spannweite in Klammern (jeweils untere Zeile) angegeben.

	3D-PDwFS	2D-PDwFS	p-value
artifacts	4.65 ± 0.67 5 (3–5)	3.65 ± 0.49 4 (3–4)	< 0.01
image sharpness	4.80 ± 0.41 5 (4–5)	4.65 ± 0.49 5 (4–5)	0.30
homogeneity of FS	4.95 ± 0.22 5 (4–5)	4.55 ± 0.5 5 (4–5)	< 0.01
overall image quality	14.40 ± 0.99 13 (11–14)	12.85 ± 0.99 13 (11–15)	< 0.01

FS: fat suppression; PDwFS: proton density-weighted fat-suppressed sequence.

▶ **Table 4** Measurements of contrast ratios (CR) in 2D- and 3D-PDwFS. The CR measurement results were higher for all investigated knee structures (ACL, PCL, and MEN) in 3D-PDwFS compared to the 2D technique. Continuous variables are given as mean±standard deviation (top line) and as the median with the range in parentheses (lower line).

▶ **Tab. 4** Messungen des Kontrastverhältnisses (CR) in 2D- und 3D-PDwFS. Verglichen mit der 2D-PDwFS waren die Ergebnisse der CR für alle gemessenen Kniestrukturen (ACL, PCL und MEN) in der 3D-PDwFS höher. Kontinuierliche Variablen werden als Durchschnitt ± Standardabweichung (jeweils obere Zeile) und als Median mit Spannweite in Klammern (jeweils untere Zeile) angegeben.

	3D-PDwFS	2D-PDwFS	p-value
CR ACL/ muscle	0.43 ± 0.36 0.55 (–0.51–0.82)	0.19 ± 0.43 0.34 (–0.53–0.87)	0.06
CR PCL/ muscle	0.67 ± 0.13 0.67 (0.36–0.86)	0.61 ± 0.24 0.67 (–0.12–0.87)	0.33
CR MEN/ muscle	0.71 ± 0.11 0.72 (0.40–0.86)	0.60 ± 0.21 0.65 (–0.07–0.86)	< 0.05

CR: contrast ratio; ACL: anterior cruciate ligament; PCL: posterior cruciate ligament; MEN: meniscus; FS: fat suppression; PDwFS: proton density-weighted fat-suppressed sequence.

all injuries could be identified both on the standard 2D PDwFS sequences and 3D PDwFS MPRs.

Discussion

Our study results demonstrate the feasibility of an isotropic 3D TSE knee sequence with CS in a clinically acceptable scan time at 1.5 T.

Several approaches have been used to optimize musculoskeletal protocols with the intention to accelerate image acquisition. For instance, variations of the DIXON method in 2D sequences were recently implemented in routine musculoskeletal protocols [21, 22]. Likewise, Bastian-Jordan et al. evaluated a 2-point DIXON sequence that achieved a slight scan time reduction with a better fat saturation at the cost of increased movement artifacts and chemical shift artifacts [23].

Studies using CS in musculoskeletal imaging are limited and there are only a few approaches implementing CS in 3D knee imaging. In addition, CS suffers from the limitation that its implementation is confined to specific sequences on scanners that depend on a specific vendor.

Several studies demonstrated the equivalence or even superiority of isotropic 3D sequences in diagnostic performance compared to conventional 2D sequences in knee imaging [2, 4, 24, 25]. Applying CS and PI, Kijowski et al. demonstrated a 30 % reduction in scan time (total scan time: 3:16 minutes) by using a 3D FSE sequence at 3 T without a decrease in diagnostic performance [18]. However, in that study an anisotropic data set was used to reduce acquisition time with a concomitant increase of blurring and an associated decrease in clarity of cartilage, meniscus, tendon, and muscle as well as significantly decreased conspicuity of knee joint pathology. Lee et al. used CS to accelerate an isotropic 3D FSE dataset of the knee [26]. With an acceleration factor of 1.5 and PI, they could reduce scan time by one-third from 7:14–8:08 minutes to 4:53–5:08 minutes. The authors found limitations in the inferior quality of cartilage–subchondral bone delineation in the CS sequences. Altahawi et al. achieved a reduction of scan time of approximately 5 minutes by applying CS with an acceleration factor of 1.5 using an isotropic 3D PD FS sequence at 3 T [19]. Compared to standard 2D sequences, the diagnostic quality of cartilage was superior and that of menisci was equivalent. However, the overall image quality as well as the evaluation of bones, ligaments, muscle, and fat was assessed as lower compared to conventional 2D sequences. No relevant diagnostic limitations were reported by Fritz et al. [8], who evaluated a 6-fold accelerated 3D TSE sequence at 3 T in an equivalent scan time. They assessed similar image quality and diagnostic performance compared to a TSE MRI standard protocol. Henninger et al. also worked out that the clinical performance of a 3D PD CS sequence with an integrated free-stop mechanism (stopping the acquisition once motion occurs) was similar to a routine fat-saturated 2D PD protocol with the advantage of a reduced scan time (05:38 minutes vs. 08:32 minutes) and proposed this sequence as a feasible sequence for the daily clinical routine [27]. By applying a 3D gradient and spin echo (GRASE) protocol versus a 3D FSE protocol, both using CS and PI, a scan time reduction of 43 % could be achieved by Cristobal-Huerta et al. [28]. In summary, studies that compare 3D imaging of the knee with CS to standard 2D sequen-

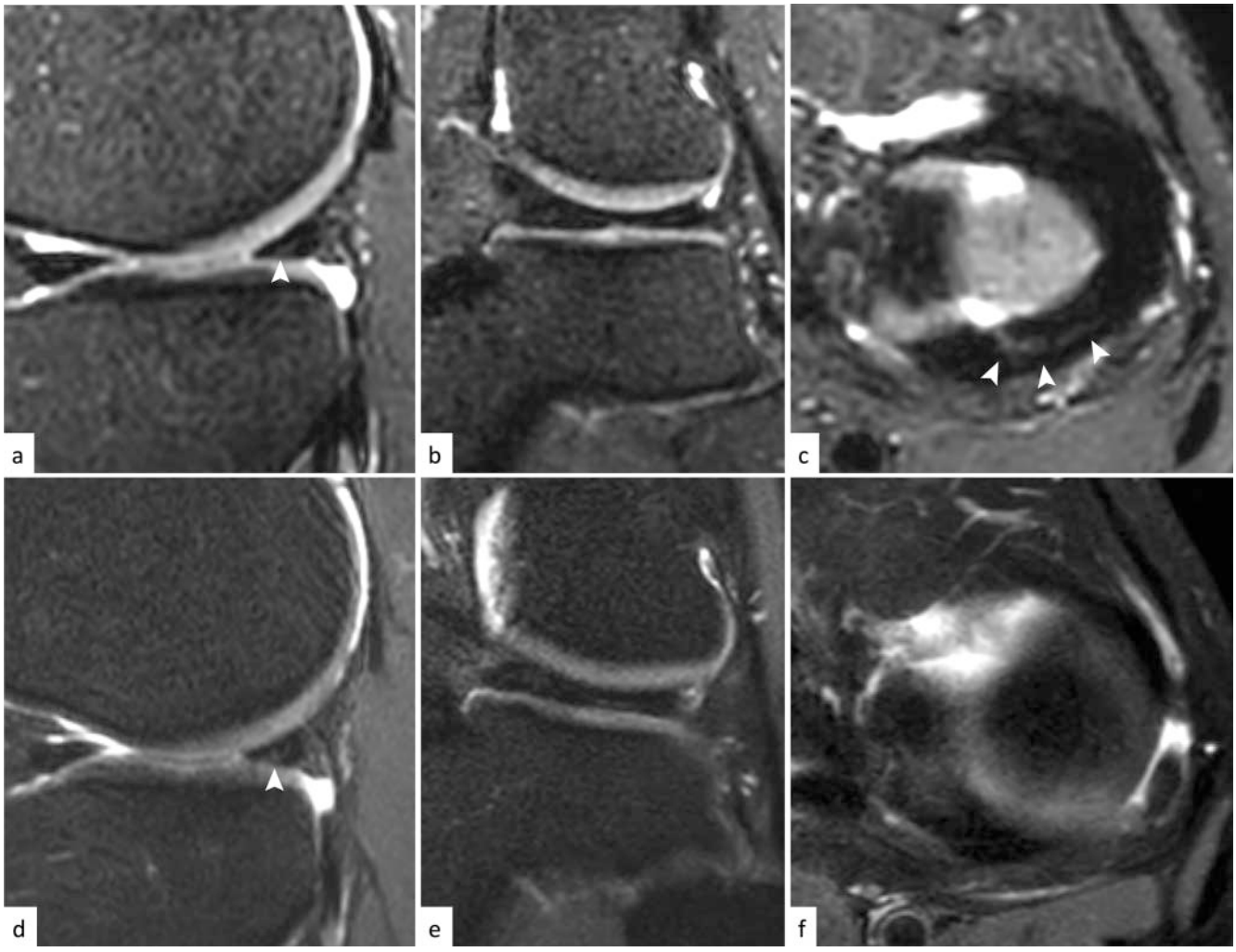

▶ **Fig. 2** Oblique meniscal tear (arrowheads) of the lateral meniscus, which can be clearly seen in the isotropic three-dimensional (3D) isotropic proton density-weighted fat-saturated sequence (PDwFS) by using multiplanar reformation. **a–c**: sagittal **a**, coronal **b**, and axial **c** reformation of the 3D PDwFS; **d–f**: sagittal **d**, coronal **e** and axial **f** two-dimensional (2D) PDwFS. Note that compared to the 2D images **d, f**, the tear can be seen in full length and clearly reaches the base of the lateral meniscus in the angulated axial **c** and sagittal **a** reformation of the 3D PDwFS, respectively.

▶ **Abb. 2** Lappenriss (Pfeilspitzen) des Außenmeniskus, welcher in der 3-dimensionalen (3D) isotropen protonengewichteten fettgesättigten Sequenz (PDwFS) eindeutig mittels multiplanarer Reformation dargestellt werden kann. **a–c** sagittale **a**, koronale **b** und axiale **c** Reformation der 3D-PDwFS; **d–f**: sagittale **d**, koronale **e** und axiale **f** 2-dimensionale (2D) PDwFS. Verglichen mit den 2D-Bildern (**d** und **f**) kann der Riss in der 3D-PDwFS in voller Länge gesehen werden und erreicht deutlich die Außenmeniskusbasis in der jeweils angulierten axialen **c** und sagittalen **a** Reformation.

ces showed similar results with slight advantages of one or the other method being reported inconsistently.

All of the abovementioned studies were performed on a 3 T MRI unit. To the best of our knowledge, no study has evaluated an isotropic 3D sequence with CS optimized for knee imaging at 1.5 T so far. With a CS acceleration factor of 8, we were able to realize a scan time of ~ 4:11 min at 1.5 T.

According to the literature, disadvantages of CS comprise image blurring, which is particularly evident in low-contrast structures, long post-processing times, and high computational burden [5, 11, 18].

However, over the last years, technical improvements that reduce these limitations have been implemented. Therefore, we did not observe these effects in our study. Especially the combination of CS and PI in addition to improved reconstruction hardware and algorithms allows for high acceleration factors with short reconstruction times. In the applied 3D sequence this is used to further shorten the echo train length and therefore to reduce TSE blurring. Tissue-specific flip angle sweep and short TR in combination with driven equilibrium provides the desired contrast while keeping the scan time short.

To evaluate diagnostic quality, we defined overall image quality as a composition of artifacts (which includes blurring), homogeneity of fat saturation, and image sharpness and could demonstrate that it was superior in the 3D sequence compared to the standard 2D sequences. That can be attributed in particular to

the lower incidence of artifacts, including blurring, pulsation and motion artifacts, and to the more homogeneous fat suppression. Image sharpness was comparable.

Studies have shown that former 3D sequences had limitations with respect to the imaging of small structures, such as the menisci. In our study, in total 16 meniscal tears could be detected – all of them in both the 2D sequences and the 3D PDwFS MPRs. In one case, a meniscal tear of the lateral meniscus adjacent to the meniscal root could only be detected clearly in the 3D sequence with the additional advantage of its ability for multiplanar reconstructions in any desired angle. All in all, no limitations regarding smaller structures were observed in our study.

Our study has limitations. With 20 patients we have a small study population. However, as this study was designed as a feasibility study and comparisons are intraindividual, the size of our study population is sufficient to demonstrate the possibility of the clinical application of the new 3D sequence. Furthermore, arthroscopic correlation is only available in 2 subjects. For the abovementioned reasons, arthroscopy was not an inclusion criterion for patient recruitment. However, as arthroscopy is considered the gold standard in verifying internal knee injuries, larger patient cohorts – preferably patients with surgery – would be desirable to further evaluate the diagnostic performance of this 3D sequence, especially concerning meniscal or chondral lesions.

In addition, the two readers were not blinded to the type of sequences that they analyzed, which could lead to some bias regarding the qualitative image analysis. However, additional quantitative data supports the qualitative findings, indicating that this defect was negligible. The detected knee injuries were evaluated by the two raters in consensus reading. For a more objective approach, a separate reading with inter- and intra-rater reproducibility testing would have been favorable.

Finally, the sequence order was not randomized, and 3D imaging was always performed last. However, as this makes movement artifacts more probable in the later sequence, this would only have led to the observation of reduced image quality in 3D imaging, which was not the case.

In conclusion, our study shows that an isotropic fat-saturated 3D PD sequence with CS enables fast and high-quality 3D imaging of the knee joint and may replace conventional multiplanar knee imaging. The detection of an additional meniscal injury indicates that besides faster image acquisition, the 3D sequence may even provide advantages in small structure imaging.

CLINICAL RELEVANCE OF THE STUDY

- Conventional 2D sequences of the knee are the current standard in knee MRI but have disadvantages like the impossibility of multiplanar reformation, which frequently results in time-consuming acquisitions of additional slice orientations
- Isotropic 3D sequences provide the possibility of multiplanar reformation, which may be favorable especially in small structure imaging
- So far, isotropic 3D sequences suffer from a prolonged scan time, which leads to an increased sensitivity for motion artifacts and thereby prevents its wide acceptance in musculoskeletal imaging
- By using compressed sensing at 1.5 T, isotropic 3D sequences of the knee can be acquired in a short scan time with high image quality and thus can replace multiplanar 2D sequences.

Conflict of Interest

Julian A. Luetkens has received lecture honoraria from Philips Healthcare.

References

[1] Homsi R, Gieseke J, Luetkens J et al. Three-Dimensional Isotropic Fat-Suppressed Proton Density-Weighted MRI at 3 Tesla Using a T/R-Coil Can Replace Multiple Plane Two-Dimensional Sequences in Knee Imaging. Fortschr Röntgenstr 2016; 188: 949–956. doi:10.1055/s-0042-111826

[2] Kudo H, Inaoka T, Kitamura N et al. Clinical value of routine use of thin-section 3D MRI using 3D FSE sequences with a variable flip angle technique for internal derangements of the knee joint at 3T. Magn Reson Imaging 2013; 31: 1309–1317. doi:10.1016/j.mri.2013.02.003

[3] Subhas N, Kao A, Freire M et al. MRI of the Knee Ligaments and Menisci: Comparison of Isotropic-Resolution 3D and Conventional 2D Fast Spin-Echo Sequences at 3 T. Am J Roentgenol 2011; 197: 442–450. doi:10.2214/Am J Roentgenol.10.5709

[4] Kijowski R, Davis KW, Woods MA et al. Knee Joint: Comprehensive Assessment with 3D Isotropic Resolution Fast Spin-Echo MR Imaging – Diagnostic Performance Compared with That of Conventional MR Imaging at 3.0 T. Radiology 2009; 252: 486–495. doi:10.1148/radiol.2523090028

[5] Garwood ER, Recht MP, White LM. Advanced Imaging Techniques in the Knee: Benefits and Limitations of New Rapid Acquisition Strategies for Routine Knee MRI. Am J Roentgenol 2017; 209: 552–560. doi:10.2214/AJR.17.18228

[6] Van Dyck P, Gielen JL, Vanhoenacker FM et al. Diagnostic performance of 3D SPACE for comprehensive knee joint assessment at 3 T. Insights Imaging 2012; 3: 603–610. doi:10.1007/s13244-012-0197-5

[7] Yao L, Pitts JT, Thomasson D. Isotropic 3D Fast Spin-Echo with Proton-Density-Like Contrast: A Comprehensive Approach to Musculoskeletal MRI. Am J Roentgenol 2007; 188: W199–W201. doi:10.2214/AJR.06.0556

[8] Fritz J, Raithel E, Thawait GK et al. Six-Fold Acceleration of High-Spatial Resolution 3D SPACE MRI of the Knee Through Incoherent k-Space Undersampling and Iterative Reconstruction – First Experience. Invest Radiol 2016; 51: 400–409. doi:10.1097/RLI.0000000000000240

[9] Kijowski R, Davis KW, Blankenbaker DG et al. Evaluation of the menisci of the knee joint using three-dimensional isotropic resolution fast spin-echo imaging: diagnostic performance in 250 patients with surgical correlation. Skeletal Radiol 2012; 41: 169–178. doi:10.1007/s00256-011-1140-4

[10] Candes EJ, Romberg J, Tao T. Robust uncertainty principles: exact signal reconstruction from highly incomplete frequency information. IEEE Trans Inf Theory 2006; 52: 489–509. doi:10.1109/TIT.2005.862083

[11] Jaspan ON, Fleysher R, Lipton ML. Compressed sensing MRI: a review of the clinical literature. Br J Radiol 2015; 88: 20150487 doi:10.1259/bjr.20150487

[12] Vasanawala SS, Alley MT, Hargreaves BA et al. Improved Pediatric MR Imaging with Compressed Sensing. Radiology 2010; 256: 607–616. doi:10.1148/radiol.10091218

[13] Feng L, Benkert T, Block KT et al. Compressed sensing for body MRI. J Magn Reson Imaging 2017; 45: 966–987. doi:10.1002/jmri.25547

[14] Zhou Y, Pandit P, Pedoia V et al. Accelerating t 1ρ cartilage imaging using compressed sensing with iterative locally adapted support detection and JSENSE. Magn Reson Med 2016; 75: 1617–1629. doi:10.1002/mrm.25773

[15] Pandit P, Rivoire J, King K et al. Accelerated T1ρ acquisition for knee cartilage quantification using compressed sensing and data-driven parallel imaging: A feasibility study. Magn Reson Med 2016; 75: 1256–1261. doi:10.1002/mrm.25702

[16] Worters PW, Sung K, Stevens KJ et al. Compressed-Sensing multispectral imaging of the postoperative spine. J Magn Reson Imaging 2013; 37: 243–248. doi:10.1002/jmri.23750

[17] Zibetti MVW, Sharafi A, Otazo R et al. Compressed sensing acceleration of biexponential 3D-T 1ρ relaxation mapping of knee cartilage. Magn Reson Med 2019; 81: 863–880. doi:10.1002/mrm.27416

[18] Kijowski R, Rosas H, Samsonov A et al. Knee imaging: Rapid three-dimensional fast spin-echo using compressed sensing. J Magn Reson Imaging 2017; 45: 1712–1722. doi:10.1002/jmri.25507

[19] Altahawi FF, Blount KJ, Morley NP et al. Comparing an accelerated 3D fast spin-echo sequence (CS-SPACE) for knee 3-T magnetic resonance imaging with traditional 3D fast spin-echo (SPACE) and routine 2D sequences. Skeletal Radiol 2017; 46: 7–15. doi:10.1007/s00256-016-2490-8

[20] Matcuk GR, Gross JS, Fields BKK et al. Compressed Sensing MR Imaging (CS-MRI) of the Knee: Assessment of Quality, Inter-reader Agreement, and Acquisition Time. Magn Reson Med Sci 2020; 19: 254–258. doi:10.2463/mrms.tn.2019-0095

[21] Maeder Y, Dunet V, Richard R et al. Bone Marrow Metastases: T2-weighted Dixon Spin-Echo Fat Images Can Replace T1-weighted Spin-Echo Images. Radiology 2018; 286: 948–959. doi:10.1148/radiol.2017170325

[22] Eggers H, Brendel B, Duijndam A et al. Dual-echo Dixon imaging with flexible choice of echo times. Magn Reson Med 2011; 65: 96–107. doi:10.1002/mrm.22578

[23] Bastian-Jordan M, Dhupelia S, McMeniman M et al. A quality audit of MRI knee exams with the implementation of a novel 2-point DIXON sequence. J Med Radiat Sci 2019; 66: 163–169. doi:10.1002/jmrs.350

[24] Lim D, Han Lee Y, Kim S et al. Clinical value of fat-suppressed 3D volume isotropic spin-echo (VISTA) sequence compared to 2D sequence in evaluating internal structures of the knee. Acta radiol 2016; 57: 66–73. doi:10.1177/0284185114567560

[25] Jung JY, Yoon YC, Kwon JW et al. Diagnosis of Internal Derangement of the Knee at 3.0-T MR Imaging: 3D Isotropic Intermediate-weighted versus 2D Sequences. Radiology 2009; 253: 780–787. doi:10.1148/radiol.2533090457

[26] Lee SH, Lee YH, Suh JS. Accelerating knee MR imaging: Compressed sensing in isotropic three-dimensional fast spin-echo sequence. Magn Reson Imaging 2018; 46: 90–97. doi:10.1016/j.mri.2017.10.018

[27] Henninger B, Raithel E, Kranewitter C et al. Evaluation of an accelerated 3D SPACE sequence with compressed sensing and free-stop scan mode for imaging of the knee. Eur J Radiol 2018; 102: 74–82. doi:10.1016/j.ejrad.2018.03.001

[28] Cristobal-Huerta A, Poot DHJ, Vogel MW et al. Compressed Sensing 3D-GRASE for faster High-Resolution MRI. Magn Reson Med 2019; 82: 984–999. doi:10.1002/mrm.27789